


Energy dissipation mechanism of annihilating reverse tilt domains for various applied voltagesTakuya Yanagimachi *National Institute of Technology, Akita College, School of Creative System Engineering, Department of Mechanical Engineering and Robotics, 1-1 Iijima, Bunkyo-cho, Akita, 011-8511, Japan*

(Received 30 October 2023; accepted 21 March 2024; published 12 April 2024)

When a voltage is applied to a uniformly aligned nematic liquid crystal, a characteristic texture designated as reverse tilt domain (RTD) appears. The RTD, surrounded by a domain wall, gradually shrinks and finally disappears. The domain wall splits into a pair of disclination lines by increase of the voltage. This work examines the energy dissipation mechanism of annihilation dynamics by ascertaining the phenomenological viscosity Γ based on experimentation. To evaluate Γ , the time dependence of curvature radius R is analyzed using an equation $R = A\sqrt{t_0 - t}$, where A is a fitting parameter. Parameter A decreased linearly with increasing applied voltage and suddenly became constant. Also, Γ was evaluated from A as a function of voltage. When the voltage reaches a critical value, Γ increased sharply to be one order of magnitude greater than that under low voltages. The critical voltage is consistent with the theoretically expected value at which the splitting of domain wall occurs. The transition of Γ is described clearly by localized deformation of the director field.

DOI: [10.1103/PhysRevE.109.044703](https://doi.org/10.1103/PhysRevE.109.044703)**I. INTRODUCTION**

In many material systems, topological defects of several kinds appear spontaneously because of the phase transition. The structure and dynamics of these defects are characterized by the broken symmetry. Well-known examples include vortex of liquid helium II, domain wall in ferromagnets, and disclination of liquid crystals. Especially in a liquid crystal (LC), these defects can be observed directly using a polarizing optical microscope. When the LC confined between two solid substrates (LC cell) is quenched from the isotropic state to the nematic, disclinations emerge [1–5]. The strength of the defect s is defined depending on the structure of the director field around the defect core. The strength s is defined as the rotations of director along a closed circle surrounding the disclination core. The value of s is experimentally determined from a image of the Schlieren texture to be $|s| = N/4$. Here the value N represents the number of dark brushes appears from the center. In an ordinal case, $s = \pm 1/2$ or ± 1 disclinations are observed. The director field including the disclination was well described in earlier works. The various boundary conditions of solid substrates or change in elastic energy because of the escape into the third dimension were discussed in [6–8].

Another method to reveal topological defects is by application of a voltage. When a nematic liquid crystal (NLC) with negative dielectric anisotropy is subjected to the vertical alignment condition, umbilical defects emerge [9,10]. The director field around umbilical defects is similar with that of $s = \pm 1$ disclinations, except for the core region. The domain wall loop also appears in the electric field [11]. Because the domain wall has excess energy, the loop shrinks and finally

ceases to exist. By combining the quenching process with the applying voltage, transformation of the domain wall structure can be observed [12]. In the nematic state without voltage, the $s = \pm 1/2$ disclinations appeared at both ends of the domain wall, called the π wall. A Brochard-Léger wall, which connects disclinations with opposite signs, is added by the application of voltage. The annihilation dynamics of $s = \pm 1/2$ disclinations is damped in the voltage.

Reverse tilt domain (RTD) appears under an external magnetic field applied to the LC cell with planar alignment [13]. In some domains, the director tilts uniformly. The boundary of domains with different tilt state is observed as the domain wall. The domain wall loop surrounding a single RTD slowly shrinks. It eventually disappears. The same domains are observed by application of voltage [14–16]. At a low voltage, the domain wall does not include the core structure, which appears in the disclinations. When the voltage becomes a certain value, approximately twice as high as the threshold of Fréedericksz transition V_c , the domain wall splits into a pair of disclination lines. This structural change is called pincement [17]. The pincement of a whole domain wall loop was observed directly under a polarizing optical microscope [14]. Also, deformation dynamics of the director field was observed [18].

In earlier works, the dynamics of RTDs were observed for various experimental conditions. Solid substrates with heterogeneity “including dust particles, substrate roughness, and nonuniform surface coverage” were introduced [15]. In addition, the various cell gaps, temperatures, and applied voltages were widely examined for an LC cell with uniform substrates [16]. Statistical properties of RTDs with random form were observed in these works. The dynamics of RTDs is successfully described by assuming the energy dissipation as a simple viscous drag force. The total size of shrinking domains was measured. The results implied that the pincement

*yanagi@akita-nct.ac.jp

influenced the time dependence of the domain size. Nevertheless, the effect of the pincement on energy dissipation mechanism remains unclear. Considering that the director re-orientation dominates the energy dissipation, pincement can be expected to change the phenomenological viscosity which the moving domain wall feels. For a clearer description, the energy dissipation mechanism and its differences before and after pincement must be elucidated by analyzing the dynamics.

The energy dissipation around the nematic disclination, which includes the core structure, was examined well in earlier studies. In a theoretical work, the energy dissipation was described by introducing the phenomenological viscous drag force [19]. Here the disclinations were assumed as moving lines in the system. The phenomenological viscosity was evaluated experimentally for an earlier study [20,21]. The energy dissipation was also regarded as the friction force acting on the disclinations [22,23]. The pincement, which induces the change in domain wall structure, is not considered for energy dissipation around the disclinations. In addition, the domain wall of RTD emerges as parallel with the solid substrates of the LC cell. The surface and confinement effects on the energy dissipation make the situation more confusing.

This report describes the effects of director field deformation, including pincement, on the energy dissipation mechanism around the domain wall of RTD. For more quantitative discussion, RTDs with a symmetric form, such as ellipse or circle, were selected. The characteristic voltage, where the annihilation dynamics changed, was detected. The director field around the domain wall was theoretically calculated. It was shown that the pincement occurred at the characteristic voltage appeared at the experiment. The phenomenological viscosity was evaluated by combining the experimentally obtained results and calculations. The relation between viscosity and applied voltage was described clearly by consideration of the localized deformation of the director field around the domain wall.

In a soft matter system, energy dissipation due to the dynamics of texture has a crucial effect on bulk rheological properties. The relationship between dynamics and rheology was previously reported for lamellar [24,25] or sponge phases [26] of lyotropic liquid crystals. In the thermotropic liquid crystals, the textures under shear were directly observed by using optical microscope for smectic A [27] and blue phases [28,29]. In these works, the averaged structure of many textures was discussed by statistical analysis. On the other hand, understanding the mechanism of energy dissipation in a controlled texture should be important as another way of approach. For this purpose, annihilation dynamics of RTD is an appropriate subject. The structure is switchable by changing the applied voltage, and the director field can be calculated numerically. In addition, we can observe the annihilating RTD directly under the polarizing optical microscope. It is expected that this research fills the gap between dynamics of texture and rheology of the macro systems.

II. EXPERIMENTAL

First, an LC cell was prepared using two ITO-coated glass substrates, and these ITO surfaces were treated by poly(vinyl

alcohol) (PVA; Fujifilm Wako Pure Chemical Corp.) 1 wt% aqueous solution using the spin-coating process (2500 rpm for 30 s). These substrates were heated for 1 h at 100 °C. After the heating process, a sandwich-type LC cell was assembled without the rubbing process. Two pieces of polyethylene films were used as the spacers. The edge of the LC cell was fixed using epoxy adhesive. The LC cell and glass substrate thicknesses were measured five times using a micrometer to estimate the cell gap d . The glass substrate thicknesses were subtracted from the total thickness of the LC cell. Then the cell gap was evaluated as $d = 16 \mu\text{m}$. We selected 4-cyano-4'-pentylbiphenyl (5CB; $T_{\text{CN}} = 24.2 \text{ }^\circ\text{C}$, $T_{\text{NI}} = 35.3 \text{ }^\circ\text{C}$) as a sample. It was purchased from Tokyo Chemical Industry Co., Ltd. Then 5CB was injected in the LC cell with capillary action at $25.0 \pm 0.2 \text{ }^\circ\text{C}$ (room temperature). The temperature had been monitored using a type E thermocouple during the experiments. Because of the flow alignment of 5CB, the uniform director field was observed under the polarizing optical microscope.

The LC cell was connected to an LCR meter (ZM2371; NF Corporation) to ascertain the critical voltage of the Fréedericksz transition V_c . The AC voltages were applied at 1 kHz to the LC cell. The capacitance C was measured as a function of the voltage. The applied voltages were changed between $0.10 \text{ V}_{\text{rms}}$ and $3.0 \text{ V}_{\text{rms}}$.

The value of V_c was estimated theoretically using the equation $V_c = \pi \sqrt{K_{11}/(\epsilon_0 \epsilon_a)}$. Here planar alignment was introduced as the boundary condition. The splay elastic constant $K_{11} = 5.1 \text{ pN}$ and dielectric anisotropy $\epsilon_a = 12.6$ were used as the material parameters of 5CB at 25 °C [30] for calculations. Here $\epsilon_0 = 8.85 \times 10^{-12} \text{ V/m}$ stands for the permittivity of vacuum. The critical voltage V_c was estimated for the system as 0.67.

To observe RTDs, the LC cell was put on the polarizing optical microscope (BM-3400TTRL; Wraymer Inc.). The top and bottom ITO-coated substrates were connected to the function generator (33500B; Agilent Technologies Inc.) to apply AC voltages of 1 kHz. The least voltage was set as $0.80 \text{ V}_{\text{rms}}$, which was greater than the theoretically estimated $V_c = 0.67 \text{ V}$. The RTD was observed at various voltages up to $3.0 \text{ V}_{\text{rms}}$ for every $0.20 \text{ V}_{\text{rms}}$.

The RTDs appeared immediately when we applied AC voltage to the cell. The loop of a domain wall shrunk. Finally, it disappeared. To verify the repeatability, observations were repeated five times for each voltage. The domain wall motion was recorded using a CCD camera mounted on the polarizing optical microscope. The movie was captured using a PC. The RTD size was measured for every 0.20 s.

III. THEORETICAL CALCULATION

A. Equation of motion for RTD

When the substrates of the LC cell are sufficiently smooth, the domain wall motion can be described as [15,16]

$$\frac{T}{R} = -\Gamma \frac{dR}{dt}, \quad (1)$$

where T represents a constant line tension, R denotes the local radius of curvature of the domain wall, and Γ expresses the phenomenological viscosity. The equation of motion indicates

the balance between elastic driving force and viscous drag. The time dependence of R is obtained by integrating the equation of motion

$$R = \sqrt{\frac{2T}{\Gamma}(t_0 - t)}, \quad (2)$$

where t_0 represents the time when the RTD finally vanishes. The values of t_0 were typically 10–30 s in our measurement system.

B. Numerical estimation of line tension

The main goal of this work is elucidating the energy dissipation process. For this purpose, Γ should be evaluated as a representative parameter of energy dissipation. The time dependence of R is obtained from the experiment. Then $\sqrt{2T/\Gamma}$ is given as a fitting parameter. To obtain Γ , we estimate tension T by numerical simulation based on the elastic theory of nematic liquid crystals [17,31].

The LC system is set as described below. We set the y axis along the direction normal to the LC cell surface. The midpoint of top and bottom surfaces is set as the origin, with the x axis set parallel to the cell surface. The angle between y axis and nematic director is defined as parameter φ . Here the director is assumed to be in the x - y plane. The director field is uniform along the z direction. The partial derivative $\partial\varphi/\partial z$ is negligible. The spatial distribution of $\varphi(x, y)$ obeys the following equation:

$$\left[\left(\frac{\partial^2 \varphi}{\partial x^2} \right) + \left(\frac{\partial^2 \varphi}{\partial y^2} \right) \right] - \frac{1}{\xi_d^2} \cos\varphi \sin\varphi = 0. \quad (3)$$

The electric coherence length ξ_d is given as $\sqrt{Kd^2/(V^2\varepsilon_0\varepsilon_a)}$. The total energy of the director field F_{total} under voltage V is given as the sum of the elastic free energy F_e and the dielectric free energy F_d , which are given as

$$F_e = \int_S \frac{1}{2} K \left[\left(\frac{\partial \varphi}{\partial x} \right)^2 + \left(\frac{\partial \varphi}{\partial y} \right)^2 \right] dS, \quad (4)$$

$$F_d = - \int_S \frac{1}{2} \varepsilon_0 \varepsilon_a \left(\frac{V}{d} \right)^2 \cos^2 \varphi dS. \quad (5)$$

To simplify the model, one constant approximation is introduced as $K = K_{11} \approx K_{22} \approx K_{33}$. The integration is performed in the xy plane, assuming that the system has unit length along the z axis.

First, total energy F_{total} without a domain wall is calculated. For this purpose, Eq. (3) is integrated numerically to find the spatial distribution of φ . Here the director field is uniform along the x direction. Also, the partial derivative $\partial^2\varphi/\partial x^2$ is removed. Equation (3) is assumed to be an ordinary differential equation. The tightly bound planar alignment condition is imposed. The boundary condition is defined simply as $\varphi = \pi/2$ at $y = \pm d/2$. Total energy $F_{\text{total}} = F_e + F_d$ is obtained using Eqs. (4) and (5).

The spatial distribution of φ including the domain wall is calculated under the suitable boundary condition. When the x value is sufficiently large, the distribution of φ approaches that without the domain wall. In addition, because of a tightly bound planar alignment, the boundary conditions at the top and bottom surfaces are the same as those without the domain

wall. The domain wall is placed along the y axis. The calculation is started from 0.6 V, which is slightly smaller than V_c . Under small voltages up to 1.8 V, the boundary condition along the y axis is

$$\varphi(0, y) = \pi/2 \quad (-d/2 \leq y \leq d/2). \quad (6)$$

When the applied voltage is sufficiently large, the domain wall structure changes into a pair of $\pm 1/2$ disclinations that appear around the top and bottom substrates [14,16]. When two disclinations are introduced into the system, the boundary condition along the y axis is

$$\varphi(0, y) = \begin{cases} \pi/2 & (d/2 - l < y \leq d/2) \\ 0 & (-d/2 + l \leq y \leq d/2 - l) \\ \pi/2 & (-d/2 \leq y < -d/2 + l) \end{cases}. \quad (7)$$

Parameter l represents the distance between LC cell surface and the disclination core. The spatial distribution $\varphi(x, y)$ including disclinations is evaluated for voltages of 1.0 V–3.0 V.

Using the boundary condition presented in this section, the director field of the $0 \leq x$ region is calculated. The left-hand side is obtainable as the mirror image of the calculated region. The total energy of system F_{total} , which includes the domain wall, is obtained using Eqs. (4) and (5).

Line tension T , which appears in Eq. (1), is equal to the energy of the domain wall per unit length. The energy is given as the difference between F_{total} with and without the domain wall. The domain wall energy is determined as ΔF_{total} . Without the disclinations, the distributions of φ and ΔF_{total} are defined uniquely. However, φ depends on parameter l when the disclinations are introduced into the system. The spatial distribution of φ and the energy ΔF_{total} are calculated for various l . When ΔF_{total} reaches the minimum, φ and $\Delta F_{\text{total}} = T$ are defined as those of the real system. In this way, the line tension is estimated numerically.

IV. RESULTS AND DISCUSSION

A. Evaluation of V_c

The capacitance C of LC cell was measured as a function of voltage. The result is shown in Fig. 1. Capacitance was almost constant from 0.1 V_{rms} to 0.6 V_{rms} . Subsequently, C sharply increased at around 0.7 V_{rms} , indicating that the molecular direction changed because of the Fréedericksz transition. The marks shown in Fig. 1 before and after the transition were fitted by dashed linear lines. The critical voltage of the Fréedericksz transition was obtained as the intersection of these lines as $V_c = 0.66 V_{\text{rms}}$. The measured value of critical voltage was the same as that of the theoretically calculated value ($= 0.67$ V) for the strong planar anchoring condition. This result indicated directly that 5CB molecules are tightly bound to be parallel with the substrates in the real LC cell.

For various voltages of 0.8–3.0 V_{rms} RTDs were observed. The voltages were higher than either the measured or calculated V_c .

B. Domain wall dynamics

Actually, RTD appeared immediately when an AC voltage was applied to the LC cell. When the voltage was removed

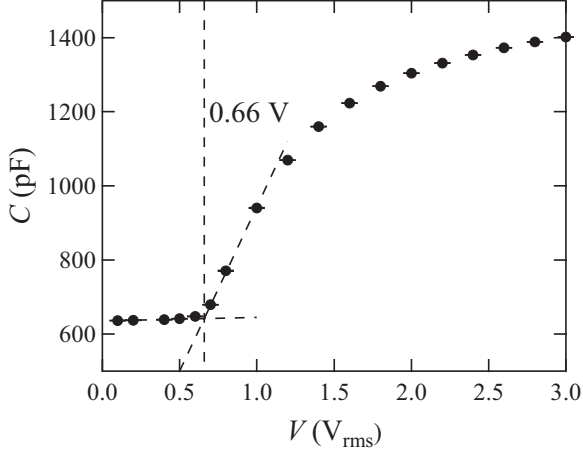


FIG. 1. Capacitance of the LC cell under 1 kHz AC voltages. The measurements were repeated 10 times. The profile shows the averaged values. The error bars are given by the standard deviation.

and applied again, RTD appeared at a similar position. The repeatability was reported earlier and was explained by the heterogeneous surface effect [15]. The shrinking RTD dynamics is shown in Fig. 2, as observed in $0.80 V_{\text{rms}}$. In the numerical calculation based on one constant approximation, the anisotropy of Frank elastic constants is ignored. However, the influence of anisotropy is clearly seen in Fig. 2. Because of the closed loop geometry, both the splay-bend and twist-bend distortions present along the loop. As a result, the RTD is elongated [13]. The lengths of minor axis a and of major axis b were obtained from images of shrinking RTD. As Fig. 2(e) shows, a circle can be fit to the domain wall. This result indicates the curvature radius of the domain wall as almost uniform, except for the cusps which appeared at both ends of major axis b . Because the driving force on the domain wall was inversely proportional to R , the uniform driving force appeared on the loop. Also, because the cusps were nothing but points on the domain wall, their contributions to the driving force were negligible.

The curvature radius R of the circle was estimated as

$$R = \frac{a^2 + b^2}{4a}. \quad (8)$$

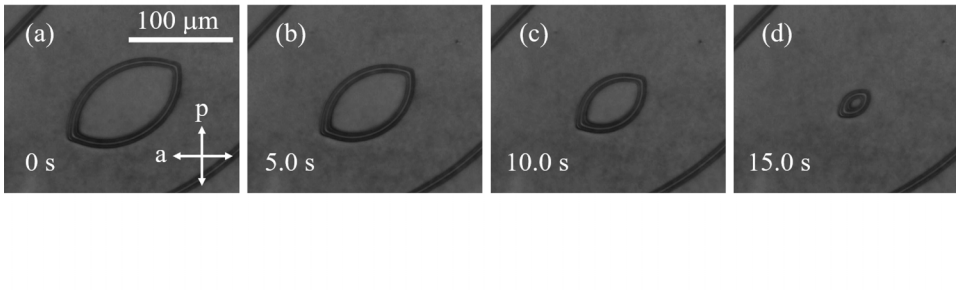


FIG. 2. Annihilation dynamics of shrinking RTD of last 15.0 s (a)–(d). Lengths of the minor axis a and major axis b were inferred from image (e). Curvature radius R was calculated from these values.

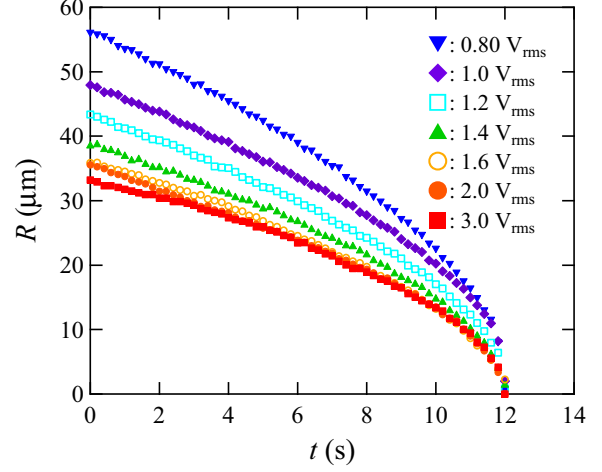


FIG. 3. Time dependence of R for various voltages ($0.80 V_{\text{rms}}$ – $3.0 V_{\text{rms}}$). The last 12.0 s of the dynamics are visible in the profiles.

As shown in Fig. 2(e), lengths a and b were estimated, respectively, as $62.5 \mu\text{m}$ and $110 \mu\text{m}$. In this case, the curvature radius R was $64.3 \mu\text{m}$.

The time course of R is shown in Fig. 3 under voltages varied from $0.80 V_{\text{rms}}$ to $3.0 V_{\text{rms}}$. For all cases, R decreased and finally reached zero, indicating that the domain wall vanished. The velocity of domain wall dR/dt was given by the slope of the profiles. The domain wall moved slowly initially. Because the driving force was inversely proportional to R , the force increased at the late stage. The domain wall accelerated. The applied voltages clearly influenced the domain wall velocity. The motion of domain wall under $0.80 V_{\text{rms}}$ was the fastest among all of the results. The velocity became slower with increasing applied voltage. When the voltage was higher than $1.6 V_{\text{rms}}$, these curves became the same.

The time dependence of R shown in Fig. 3 apparently obeys the square-root time law. This tendency is consistent with the theoretically expected time dependence presented in Eq. (2). It was reported earlier in the literature that Eq. (2) is useful for a uniform LC cell surface [15,16]. To check the usefulness of Eq. (2), the experimentally obtained results were analyzed using a function $R = A(t_0 - t)^{\nu}$ as a fitting curve. Because the last 12 s were picked up in Fig. 3, the value t_0 was set as

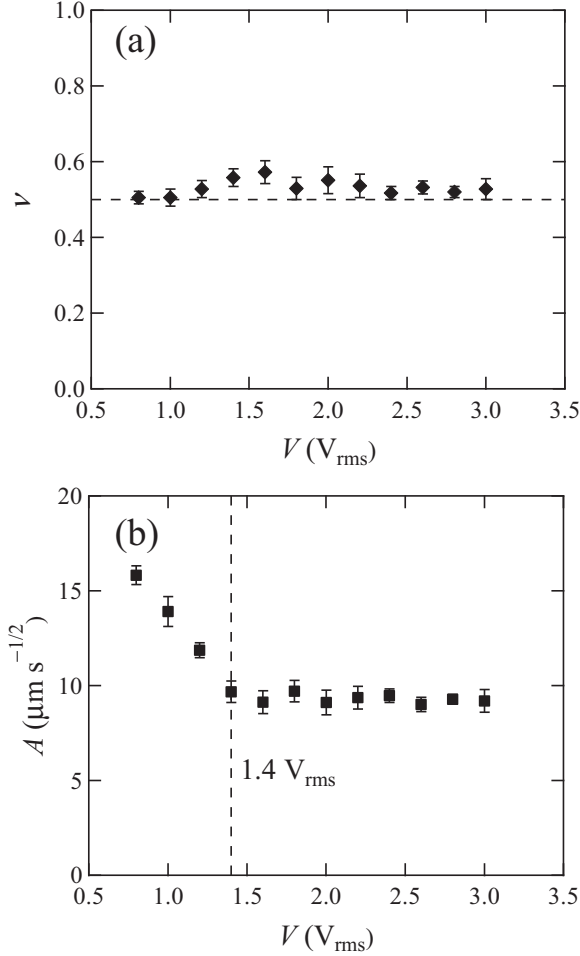


FIG. 4. Fitting parameters ν (a) and A (b) as a function of voltage. Observations were repeated for five times for each voltage. The error bars show standard deviations.

12.0 s. The exponent ν and the coefficient A were evaluated as fitting parameters. Figure 4(a) shows ν as approximately 0.5, irrespective of the applied voltage. This result indicated that Eq. (2) is applicable in our system, and indicated that the cell surface is sufficiently uniform. In addition, constant ν implies that the dynamics are phenomenologically described by Eq. (1). The change in applied voltages did not influence the basic mechanism of the domain wall motion.

Fitting parameter A equals $\sqrt{2T/\Gamma}$, which appears in Eq. (2). Figure 4(b) presents parameter A as a function of voltage. Actually, A was the largest at $V = 0.8 V_{\text{rms}}$. Its value decreased linearly and became constant when the voltage was higher than $1.4 V_{\text{rms}}$. Considering the fact that A includes line tension T , the bending on profile Fig. 4(b) might be explained by the change in director field: so-called pincement. To evaluate Γ from A , the line tension T before and after pincement is required.

C. Line tension estimated using elastic theory

The energy of the director field with and without the domain wall is calculated. The difference between them is defined as ΔF_{total} . When the domain wall including

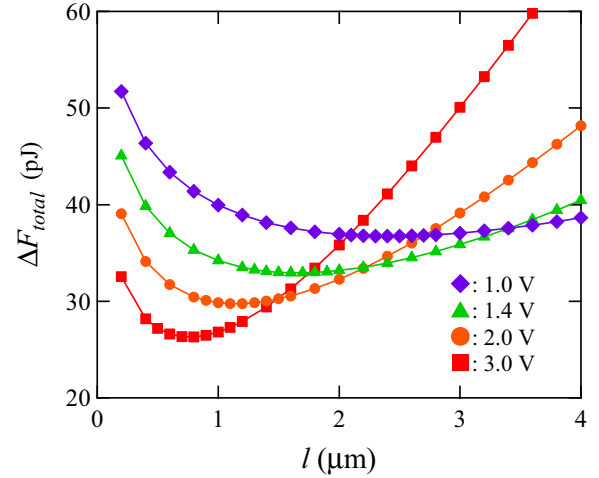


FIG. 5. Energy of the domain wall, which includes a pair of disclinations, is defined as a function of l .

disclination lines is analyzed, ΔF_{total} is given as a function of parameter l .

The relation between ΔF_{total} and l is shown in Fig. 5. Here l changes roughly by $0.2 \mu\text{m}$. The energy is estimated. More detailed calculations are performed around the energy minimum. ΔF_{total} are evaluated for every $0.1 \mu\text{m}$ of l . In Fig. 5 a shallow minimum is apparent at around $2.4 \mu\text{m}$ in $V = 1.0 \text{ V}$. The minimum value of ΔF_{total} decreases with increasing voltage, indicating that the director field becomes energetically stable under the high voltages. Because the minimum ΔF_{total} equals line tension T , the driving force acting on the domain wall decreases. In addition, the position of disclination shifts to the cell surface. In this way, the minimum value of ΔF_{total} , which is assumed to be the line tension of the real system, is obtained. The distribution of the angle φ , which gives the minimum energy, is also defined.

The spatial distributions of φ under various voltages are shown in Fig. 6. Figures 6(a)–6(d) show the domain walls without disclinations. The director fields around the top and bottom substrates are parallel to them. Here the value of φ is equal to $\pi/2 \approx 1.6$. The distribution of φ along the y axis is the same as that on the surface. The top and bottom surfaces are connected by the domain wall. The domain wall thickness along the x direction is dominated by the balance between elastic and dielectric torque. When φ is calculated in $V = 0.8 \text{ V}$, which is slightly larger than V_c of the Fréedericksz transition, the dielectric torque is small. As a result, the director field of planar alignment is more or less stable. The domain wall is thick. The domain wall thickness decreases with increasing applied voltage. The deformed director field is localized in the narrow region around the domain wall. Also, φ changed sharply between 0 and $\pi/2$, as shown in Figs. 6(c) and 6(d).

The spatial distributions of φ around the domain wall with disclinations are shown in Figs. 6(e)–6(h). The director field is optimized to obtain the least ΔF_{total} for the given voltages. Because the voltage is applied between top and bottom substrates, the electric field in the LC cell is parallel to the y axis. The spatial distribution around the y axis equals zero,

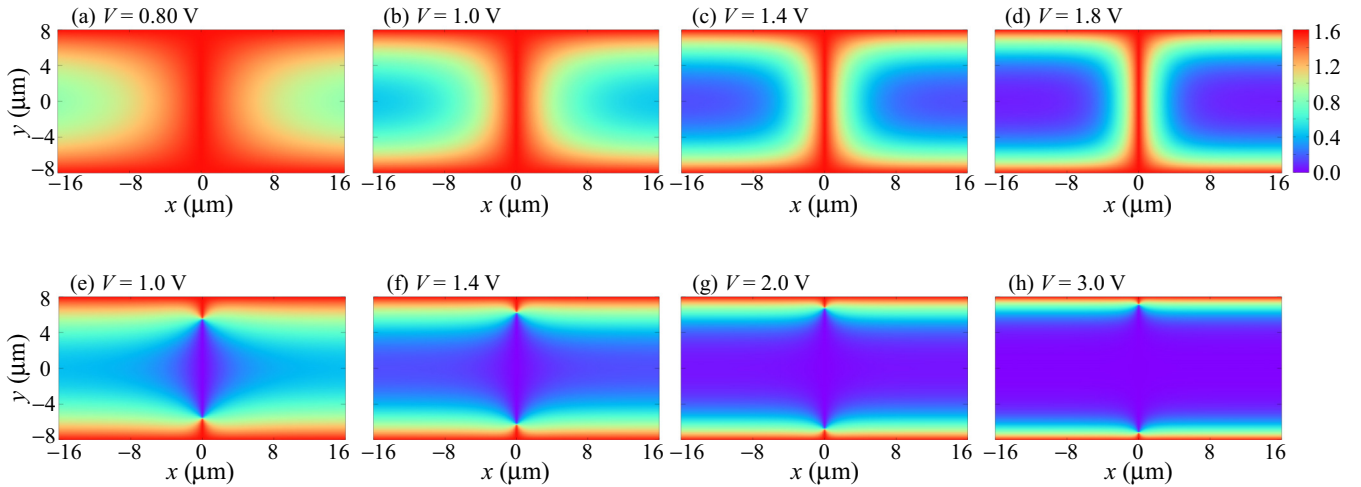


FIG. 6. Spatial distribution of the φ around the domain wall. The values of φ without disclinations are calculated for voltages of 0.80–1.8 V [(a)–(d)]. φ including a pair of disclinations are also obtained for voltages of 1.0–3.0 V. Because of the planar alignment, φ is $\pi/2$ on the top and bottom substrates. The boundary conditions along the y axis are given by Eqs. (6) and (7). The distribution of φ approaches that without the domain wall when the $|x|$ is sufficiently large.

indicating that the director between disclinations is parallel with the electric field. Under $V = 1.0$ V, the region of $\varphi = 0$ is localized around the y axis. This region spreads with increasing applied voltage. When the voltage is higher than 2.0 V, the spatial distribution of φ in the bulk region becomes uniform. The dynamics accompanies director reorientation, which is localized around the disclinations.

Based on theoretical calculations, the energies of a domain wall with and without disclinations are obtained. The energy ΔF_{total} is presented in Fig. 7 as a function of voltage. The square dots represent ΔF_{total} of the defect-free domain wall. The value of energy becomes approximately 0 in $V = 0.6$ V, indicating that the director field does not deform at this voltage. The result is consistent with the fact that $V = 0.6$ V is smaller than the critical voltage V_c . The energy ΔF_{total} shown by square dot increases linearly between 0.8 V and 1.8 V. The ΔF_{total} of the domain wall, including the disclination pair,

is shown by the circular dots in the figure. The energy was calculated between $V = 1.0$ V and 3.0 V. The value gradually decreases concomitantly with increasing voltage. The energy curve crosses with that without disclinations. The intersection of energy curves appeared between 1.4 V and 1.6 V. Because the structure which gives the minimum energy appears in the real system, Fig. 7 shows that the transition of director field emerges at around 1.4 V. In other words, pincement occurs at around the intersection of ΔF_{total} . This voltage of the intersection is consistent with the critical value shown in Fig. 4(b), where A becomes constant. In this way, the critical voltage of pincement is definable clearly based on the experiment results by analysis of the annihilation dynamics of the domain wall loop.

The static distribution of φ is calculated with applying the boundary condition shown in Eqs. (6) and (7). Considering the

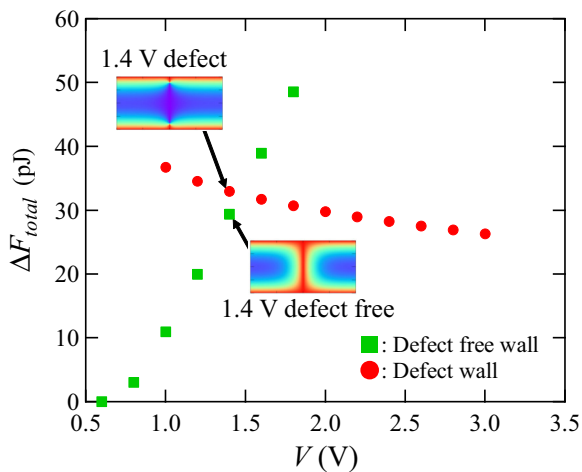


FIG. 7. Energy ΔF_{total} estimated by calculation. Energy of the domain wall with and without disclinations crosses between 1.4 V and 1.6 V. Pincement is expected to occur at the intersection.

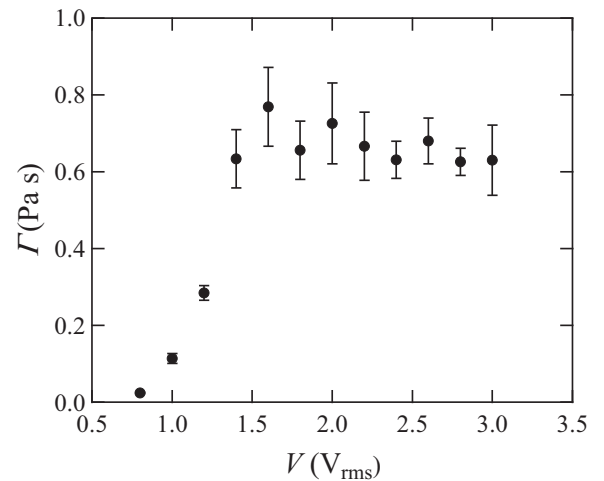


FIG. 8. Relation between Γ and applied voltage. Γ increased sharply between 0.8 V_{rms} and 1.4 V_{rms} , and became constant at the high voltage.

fact that the velocity of domain wall is slow enough, the director field around moving domain wall can be approximated by the static one. Similar approximation was introduced for analyzing the interaction between moving disclinations [2–5]. The energy of disclination core is also neglected. The core energy is estimated to be $\pi s^2 K$ [6]. When the core energy is added to Fig. 7, the energy of defect wall increases roughly 5 pJ. The shift is small compared to the energy of bulk director field, and the energy ΔF_{total} and threshold voltage of pincement do not change so much. If the domain wall of RTD is confined in a quite thin LC cell, the core energy may have a fundamental contribution to the system. In that situation, the energy of the system should be evaluated by using Q -tensor theory [18], which can introduce the core structure suitably.

D. Energy dissipation in the LC cell

Parameter A of Fig. 4(b) was found by experimentation. The parameter is defined as $A = \sqrt{2T/\Gamma}$. The value of T is estimated from the theoretical calculation presented in Fig. 7. Γ is evaluated by combining the results shown in Figs. 4 and 7, to obtain $\Gamma = 2T/A^2$. The value of Γ is presented in Fig. 8 as a function of the applied voltage. Γ at $V = 0.8 V_{\text{rms}}$ is 0.024 ± 0.001 Pa s, which is of similar order with the rotational viscosity $\gamma_1 = 0.08$ Pa s at $T = 26^\circ\text{C}$ [32]. It is shown in Fig. 6 that the domain wall width is large at low voltage. The director field does not differ greatly from the uniform planar alignment. The director in the LC cell reorients slowly and uniformly when the domain wall moves. The energy dissipation dynamics are expected to be similar with that of the bulk liquid crystal under viscosity measurements. Results show that the evaluated parameter Γ is consistent with γ_1 measured for the bulk 5CB.

Γ sharply increases in the voltages between $0.8 V_{\text{rms}}$ and $1.4 V_{\text{rms}}$, where the domain wall does not include disclinations. Figures 6(a)–6(d) show that the domain wall becomes narrow with increasing voltage. Because the deformation is localized in the high voltage, the director field quickly reorients because of the domain wall dynamics. The quick motion of the director field induces the large dissipation of energy. Consequently, the evaluated value of Γ increases. Γ of $1.4 V_{\text{rms}}$ is one order of magnitude larger than that of $0.8 V_{\text{rms}}$.

The electrorheological effect of 5CB was checked to explain the increasing of Γ . The increase of bulk viscosity with voltage is known as the electrorheological effect [33]. In earlier work, viscosity increased by application of an AC voltage of 1 kHz. The electric field strength was $1 \text{ kV}_{\text{rms}}/\text{mm}$. The difference in viscosities measured with and without electric field was roughly 0.07 Pa s. However, Γ for our system changed drastically by 0.7 Pa s under $0.09 \text{ kV}_{\text{rms}}/\text{mm}$ ($1.4 V_{\text{rms}}$ over $d = 16 \mu\text{m}$). The change in Γ is too large to be explained by the electrorheological effect of the bulk 5CB. Noting that some dissipation modes, such as the effect of shear viscosity and backflow, are neglected. The simple discussion in this work tells only that the change in Γ is not explained by the bulk viscosity of 5CB.

For more quantitative discussion, the energy dissipation around the domain wall is numerically calculated. The energy dissipation in a unit time is obtained for the product of viscous drag force and velocity, to be Γv^2 . Here v is the velocity of

domain wall, and the motion is assumed to be quasistatic. On the other hand, the energy dissipation is also defined from the reorientation of director field [19,31]. Because the energy dissipation from director reorientation is consistent with that from viscous drag force, Γ is obtained by the following equation:

$$\Gamma v^2 = \gamma_1 \int_S \left(\frac{\partial \varphi}{\partial t} \right)^2 dS = \gamma_1 \int_S \left(\frac{dx}{dt} \right)^2 \left(\frac{\partial \varphi}{\partial x} \right)^2 dS. \quad (9)$$

The contribution of shear viscosity and backflow is neglected in this equation. The domain wall moves toward the x direction, and dx/dt equals to v . Then Γ is obtained to be

$$\Gamma = \gamma_1 \int_S \left(\frac{\partial \varphi}{\partial x} \right)^2 dS. \quad (10)$$

Based on Eq. (10) and the distribution of φ seen in Fig. 6, the values of Γ are numerically evaluated as between 0.050 Pa s ($0.8 V$) and 0.46 Pa s ($1.4 V$). These theoretical values are consistent with those shown in Fig. 8. The sharp increase of Γ is also seen from the numerical calculation.

Γ becomes constant at voltages greater than $1.6 V_{\text{rms}}$. The domain wall includes disclinations under these voltages. The phenomenological viscosity was estimated theoretically as

$$\Gamma = 2\pi \gamma_1 s^2 \ln(L/r_c). \quad (11)$$

The factor 2 represents that both disclination lines around the top and bottom surfaces contribute to the energy dissipation. Here $s = \pm 1/2$ represents the strength of disclinations, L denotes the system size, and r_c stands for the core radius [20,21]. Equation (11) is defined for the disclination in a bulk liquid crystal. Because the domain wall of our system is confined between two surfaces, the maximum value of L equals the cell gap $d = 16 \mu\text{m}$. By applying voltage, the size of deformed region around a disclination is given as ξ_d . Considering the fact that the director reorientation progressed in this deformed region, ξ_d is also available as the effective size of the system. The ξ_d are evaluated to be $2.1 \mu\text{m}$ ($1.6 V_{\text{rms}}$) and $1.1 \mu\text{m}$ ($3.0 V_{\text{rms}}$), respectively. Since these values of ξ_d are smaller than the cell gap, the values are acceptable as the effective size of the system. The representative value of r_c was $0.01 \mu\text{m}$ [3]. In this situation, the theoretical value of Γ was estimated as between 0.7 Pa s ($1.6 V_{\text{rms}}$) and 0.6 Pa s ($3.0 V_{\text{rms}}$). The values of Γ for the systems including disclinations were also evaluated from the numerical simulation, based on Eq. (10). The values were 0.48 Pa s ($1.4 V$) and 0.38 Pa s ($3.0 V$), respectively. These values discussed in this section were roughly consistent with those shown in Fig. 8, indicating that the increase of Γ was explained successfully by the generation of disclination lines caused by the pincement.

In Figs. 6(e)–6(h), deformation caused by disclination is localized around the substrates, especially at high voltages. Energy dissipation at the cell middle is negligible because the director field is uniform in this region. Here the distance between disclination and cell surface l is obtained by minimizing ΔF_{total} . The value of optimized l is roughly $1 \mu\text{m}$. The value is one order of magnitude smaller than the cell gap d . Therefore, Γ at high voltages corresponds to the viscosity of 5CB under the influence of the cell surface. As advanced work along this avenue of research, it is expected that the surface

roughness and its effects on the dynamics of domain wall can be detected by evaluating Γ .

V. CONCLUSIONS

For this work, the dynamics of RTD surrounded by domain wall loop was observed under a polarizing optical microscope. After the annihilation dynamics was recorded using a CCD camera, the curvature radius R was obtained as a function of time. Equation (2) was applied to the experimentally obtained result. Thereby, $A = \sqrt{2T/\Gamma}$ was obtained as a fitting parameter. A plot of A vs applied voltage V shows clearly that the tendency of A clearly switched at $V = 1.4 V_{\text{rms}}$.

To evaluate the parameter Γ , which characterized the energy dissipation, the line tension T was calculated numerically. The line tension was obtained as the energy of domain wall per unit length ΔF_{total} . Both ΔF_{total} with and without a pair of disclination lines were estimated. They are shown in Fig. 7. The results clearly illustrate that the change in the director field, so-called pincement, occurs between $V = 1.4 V$ and $1.6 V$. The voltage was consistent with the critical value shown in Fig. 4(b).

The value of Γ was evaluated using theoretically estimated T before and after pincement. The findings indicate that Γ increased sharply between $V = 0.8 V_{\text{rms}}$ and $1.4 V_{\text{rms}}$

because of the localization of director field deformation. When the voltage was greater than $1.6 V_{\text{rms}}$, Γ was constant and large: approximately 0.7 Pa s . Based on theoretically obtained results, disclinations were introduced to the domain wall. Energy dissipation was localized around the disclinations.

In this way, energy dissipation process of domain wall dynamics was characterized by combining findings from experimentation and theoretical calculation. Results show that the localized deformation of director field has a crucially important role for elucidation of the dissipation mechanism. We expect that similar method can be applicable for investigating the LC confined between rough surfaces, or for other complex systems such as liquid crystalline lubricants.

ACKNOWLEDGMENTS

T.Y. thanks Prof. Akihito Hibara and Dr. Motohiro Kasuya. The experimental equipment such as the polarizing optical microscope and LCR meter are due to their kind support. T.Y. is grateful to Prof. Kazuya Saito and Dr. Yasuhisa Yamamura for critical advice about temperature measurement and control systems. This research is supported in part by the Foundation for Japanese Chemical Research (511R) and by a Grant-in-Aid for Scientific Research (C) (JP23K03597).

-
- [1] W. Brinkman and P. Cladis, *Phys. Today* **35**(5), 48 (1982).
 - [2] K. Minoura, Y. Kimura, K. Ito, R. Hayakawa, and T. Miura, *Phys. Rev. E* **58**, 643 (1998).
 - [3] A. Bogi, P. Martinot-Lagarde, I. Dozov, and M. Nobili, *Phys. Rev. Lett.* **89**, 225501 (2002).
 - [4] C. Blanc, D. Svenšek, S. Žumer, and M. Nobili, *Phys. Rev. Lett.* **95**, 097802 (2005).
 - [5] T. Yanagimachi, S. Yasuzuka, Y. Yamamura, and K. Saito, *J. Phys. Soc. Jpn.* **81**, 034601 (2012).
 - [6] M. Kleman and O. D. Lavrentovich, *Soft Matter Physics: An Introduction, 2003rd ed.* (Springer, New York, 2002).
 - [7] P. Cladis and M. Kléman, *J. Phys. France* **33**, 591 (1972).
 - [8] L. Radzihovsky and Q. Zhang, *Phys. Rev. E* **79**, 041702 (2009).
 - [9] I. Dierking, O. Marshall, J. Wright, and N. Bulleid, *Phys. Rev. E* **71**, 061709 (2005).
 - [10] I. Dierking, M. Ravník, E. Lark, J. Healey, G. P. Alexander, and J. M. Yeomans, *Phys. Rev. E* **85**, 021703 (2012).
 - [11] J. Nehring, *Phys. Rev. A* **7**, 1737 (1973).
 - [12] A. Vella, R. Intartaglia, C. Blanc, I. I. Smalyukh, O. D. Lavrentovich, and M. Nobili, *Phys. Rev. E* **71**, 061705 (2005).
 - [13] L. Léger, *Mol. Cryst. Liq. Cryst.* **24**, 33 (1973).
 - [14] A. Stieb, G. Baur, and G. Meier, *J. Phys. Colloques* **36**, C1-185 (1975).
 - [15] D. K. Shenoy, J. V. Selinger, K. A. Grüneberg, J. Naciri, and R. Shashidhar, *Phys. Rev. Lett.* **82**, 1716 (1999).
 - [16] Y. Shen and I. Dierking, *J. Mol. Liq.* **313**, 113547 (2020).
 - [17] P. G. de Gennes and J. Prost, *The Physics of Liquid Crystals*, 2nd ed. (Clarendon Press, Oxford, 1993).
 - [18] A. de Lózar, W. Schöpf, I. Rehberg, D. Svenšek, and L. Kramer, *Phys. Rev. E* **72**, 051713 (2005).
 - [19] G. Ryskin and M. Kremenetsky, *Phys. Rev. Lett.* **67**, 1574 (1991).
 - [20] A. Mertelj and M. Čopič, *Phys. Rev. E* **69**, 021711 (2004).
 - [21] N. Osterman, J. Kotar, E. M. Terentjev, and P. Cicuta, *Phys. Rev. E* **81**, 061701 (2010).
 - [22] C. Blanc, A. Vella, M. Nobili, and P. Martinot-Lagarde, *Mol. Cryst. Liq. Cryst.* **438**, 175/[1739] (2005).
 - [23] C. Blanc, M. Nespoulous, E. Angot, and M. Nobili, *Phys. Rev. Lett.* **105**, 127801 (2010).
 - [24] M. Berni, C. Lawrence, and D. Machin, *Adv. Colloid Interface Sci.* **98**, 217 (2002).
 - [25] J. Yamamoto and H. Tanaka, *Phys. Rev. Lett.* **74**, 932 (1995).
 - [26] L. Porcar, W. A. Hamilton, P. D. Butler, and G. G. Warr, *Phys. Rev. Lett.* **89**, 168301 (2002).
 - [27] S. Fujii, S. Komura, and C.-Y. D. Lu, *Materials* **7**, 5146 (2014).
 - [28] R. Sahoo, O. Chojnowska, R. Dabrowski, and S. Dhara, *Soft Matter* **12**, 1324 (2016).
 - [29] R. Sahoo and S. Dhara, *Fluids* **3**, 26 (2018).
 - [30] C. Maze, *Mol. Cryst. Liq. Cryst.* **48**, 273 (1978).
 - [31] P. Biscari and T. Sluckin, *SIAM J. Appl. Math.* **65**, 2141 (2005).
 - [32] H. Kneppel, F. Schneider, and N. Sharma, *J. Chem. Phys.* **77**, 3203 (1982).
 - [33] K. Negita, *J. Chem. Phys.* **105**, 7837 (1996).